Carbohydrate Polymers 316 (2023) 120996

Contents lists available at ScienceDirect

Carbohydrate Polymers

journal homepage: www.elsevier.com/locate/carbpol

Characterizing lignin-containing microfibrillated cellulose based on water interactions, fibril properties, and imaging

Xiaoxue Zhang [a,b], Peter Kitin [b], Umesh P. Agarwal [b], Rolland Gleisner [b], J.Y. Zhu [b,*]

[a] Jiangsu Co-Innovation Center of Efficient Processing and Utilization of Forest Resources, Jiangsu Provincial Key Lab of Pulp & Paper Science & Technology, Nanjing Forestry University, Nanjing 210037, China
[b] USDA Forest Products Laboratory, Madison 53726, USA

ARTICLE INFO

Keywords:
Lignin-containing microfibrillated cellulose
Mechanical fibrillation
Water retention value
Suspension stability
Cellulose crystallinity

ABSTRACT

Morphological characterization of microfibrillated cellulose (MFC) is critically important to process control in production and product specification for trade and product development yet is extremely difficult. This study evaluated several indirect methods for relative comparison of the morphology of lignin-free and lignin-containing ((L)MFCs). The (L)MFCs studied were produced using a commercial grinder through different passes from a dry lap bleached kraft eucalyptus pulp, a virgin mixed (maple and birch) unbleached kraft hardwood pulp, and two virgin-unbleached kraft softwood (loblolly pine) pulps with one bleachable grade (low lignin content) and one liner grade (high lignin content). The (L)MFCs were indirectly characterized using techniques based on water interactions, i.e., water retention value (WRV) and fibril suspension stability, as well as fibril properties, i.e., cellulose crystallinity and fine content. Optical microscopy and scanning electron microscopy were also applied to directly visualize the (L)MFCs to provide some objective measure of the morphology of the (L)MFCs. The results indicate that most measures such as WRV, cellulose crystallinity, fine content cannot be used to compare (L)MFCs from different pulp fibers. Measures based on water interactions such as (L)MFC WRV and suspension stability appeared can provide some degree of indirect assessment. This study provided the utilities and limits of these indirect methods for relative comparison of the morphologies of (L)MFCs.

1. Introduction

Rising environmental concerns have sparked a global push for advanced materials research. Cellulose is the most abundant renewable natural biopolymer on the planet, and its renewability and material properties make it a viable alternative to plastics from petroleum (Kaeb & General, 2009). Microfibrillated cellulose (MFC) is a low-cost, new type of cellulose material derived from plant biomass fibers through mechanical fibrillation with significantly increased specific surface area and thereby, water absorption capacity and accessibility of the substructural microfibrils to other materials for further processing (Li et al., 2021). MFC was first obtained by Turbak in 1983 who discussed its potential in industrial applications (Turbak et al., 1983). After decades of development, MFC is now being used as polymer reinforcement for packaging and light-weight composites, as rheology modifier in food, in cement, coatings, and paints, as barrier layer for food-contact packaging, and as water absorbent for various purposes (Klemm et al., 2011; Lavoine et al., 2012; Nassiri et al., 2021).

Various approaches for preparing MFC from plant sources have been well reviewed (Siró & Plackett, 2010). Pure mechanical fibrillation remains preferred approach to avoid any complications associated with chemical treatments. As with any new materials, proper characterization of MFC is essential for process control in production, specification for trade and product development, and of course, for product safety evaluation (Moon et al., 2023). However, the characterization of MFC is challenging, due to extensive fibril branching and high flexibility for entanglement and flocculation in suspension along with extremely high aspect ratios (Moon et al., 2023; Pöhler et al., 2010). MFCs contain fibrils with scales varying several orders of magnitude, which makes characterization difficult using existing techniques. Light diffraction which has been widely used for characterizing low aspect ratio individually separated particles cannot be used due to MFC's fibrillar network structure. Imaging methods such as optical microscopy (OM), scanning electron microscopy (Raj et al., 2016), atomic force

* Corresponding author.
E-mail address: junyong.zhu@usda.gov (J.Y. Zhu).

https://doi.org/10.1016/j.carbpol.2023.120996
Received 16 February 2023; Received in revised form 25 April 2023; Accepted 5 May 2023
Available online 10 May 2023
0144-8617/Published by Elsevier Ltd.

microscopy (AFM), and transmission electron microscopy (TEM) are the most direct way to visualize MFC morphology and have been widely applied. These methods have provided excellent understanding the complex morphological structure (Kangas et al., 2014; Singh et al., 2020; Wang, Zhu, et al., 2012). However, imaging methods cannot provide quantitative and comparative parameters for MFC because of the network and branching structural issues (Kangas et al., 2014; Moon et al., 2023). Microscopic imaging evaluation is also time-consuming and requires analysis of a great number of images to obtain statistically meaningful information.

Classification is another direct method for characterizing MFCs. Tube flow fractionation technique initially applied to papermaking fibers (Laitinen, Kemppainen, Stoor, & Niinimäki, 2011) has been applied to classify MFCs (Laitinen & Niinimaki, 2014). Results show that MFCs can be effectively fractionated according to their overall fibril sizes. The authors used SEM images and laser diffraction analysis to confirm the validity of their fractionation method. Ultracentrifugation is a method similar to classification to physically fractionate MFC. However, quantifying the size of each fraction remains a challenge for both these methods (Kangas et al., 2014).

Some indirect methods including suspension-optical transmittance, viscosity, water retention value (WRV), suspension sendimention, cellulose degree of polymerization and crystallinity have been used for characterizing MFCs (Gu et al., 2018; Kangas et al., 2014; Singh et al., 2020; Wang, Zhu, et al., 2012). Transmittance measurements can differentiate various bleached nanocellulose samples (Saito et al., 2006). Characteristics such as fibril size, fibril aggregation, and sample concentration are the key contributors to suspension-optical transmittance, but fibril color and refractive indices can also significantly affect the light transmittance of lignocellulose suspensions. Therefore, the transmittance method is not suitable for characterizing lignin containing MFCs (LMFCs) due to the color of lignin. Similarly, rheological properties are not suitable for characterizing LMFCs, because the rheology of lignocellulosic suspensions not only depend on fibril morphology, but also, on hydrophilicity and chemistry of fibril surface. Apparently, lignin in different LMFCs have different surface properties.

Cellulose is inherently hydrophilic and has strong interactions with water, which gives cellulose products great water absorbing capacity (Perkins & Batchelor, 2012). This water absorbing capacity is dependent upon the water-accessible area of cellulose. Mechanical fibrillation can substantially increase the cellulose surface area which increases its water absorbing capacity. WRV is a measure of water absorbing capacity of cellulosic fibers and can be determined using several standard methods. It is a measure of a cellulosic sample accessibility using water as the probe molecule (Luo & Zhu, 2011). WRV can be a semi-quantitative measure of the total surface area of a cellulose sample. This measurement was found to correlate to enzymatic saccharification of the substrate cellulose (Luo & Zhu, 2011; Turbak et al., 1983; Weiss et al., 2018) because it can be a measure of accessibility to cellulase (Wang, He, et al., 2012). Turbak's initial work suggested that WRV of MFCs increased with the extent of fibrillation (Turbak et al., 1983). Our earlier study also demonstrated the potential of using WRV for characterizing the degree of fibrillation using a bleached eucalyptus kraft pulp (Gu et al., 2018). However, most cellulosic materials used for producing MFC contains lignin. Lignin is known to be hydrophobic, and its hydrophobicity is affected by the delignification process employed. For example, sulfonated or carboxylated lignin can be highly hydrophilic, therefore, substrate lignin content and its chemical structure can affect a sample's WRV. Furthermore, wood species can also affect WRV as different wood can have very different pore structures and different spatial distributions of chemical components. Therefore, the utility of WRV to characterize MFCs produced from different fiber sources, especially LMFCs needs to be evaluated in order to use WRV as a process control measure for MFC production and for product specification.

Fibril aqueous suspension sedimentation or stability is another measure of fibril interaction with water. It has been used to characterize MFCs because of the relationship between fibril size, aggregates and stability (Butchosa & Zhou, 2014; Guimaraes, Botaro, et al., 2015; Silva et al., 2021a). Certainly, suspension sedimentation is also affected by fibril surface chemistry and hydrophilicity. Cellulose crystallinity (CrI) has also shown excellent sensitivity to fibrillation, especially in the microfibrillation regime (Wang, Zhu, et al., 2012). One of the advantages is that with the appropriate choice of the methods the cellulose CrI estimations are hardly affected by lignin (Agarwal, 2022; Agarwal et al., 2013; Agarwal et al., 2018). Alternatively, lignin can be removed using a mild method prior to carrying out the CrI measurement.

The objective of the present study is to evaluate several indirect measures, i.e., cellulose crystallinity, WRV, fine content, MFC suspension sedimentation stability, for characterizing MFCs. The MFCs were produced from both hardwood and softwood fibers that have different lignin contents. These characterizations will be verified with both optical and scanning electron microscopic imaging to illustrate the utility, validity, and limits of these indirect characterization methods. The goal of the study is to find simple and relatively fast method that can provide comparisons of different MFCs for industry and regulatory applications.

2. Materials and methods

2.1. Materials

Four commercial wood pulps were used for the present study. A dry lap bleached kraft eucalyptus pulp (BEP) from Fibria (Aracruz, Brazil) was soaked in distilled water at solid consistency of 10 % for 24 h, and then fiberized using a lab disintegrator (TMI, Ronkonkoma, NY). A virgin unbleached mixed hardwood (maple and birch) pulp (UHP) and two virgin unbleached softwood (loblolly pine) kraft pulps of one bleachable grade (low lignin content, USP-L) and another for liner grade (high lignin content, USP-H) were all directly shipped in wet form from commercial pulp mills in the US. The chemical compositions of the four pulp samples were analyzed (Table S1). USP-H was refined to 600 mL Canadian Standard Freeness (CSF, slightly under refined) and substituted with 15 % MFCs or a highly refined pulp (CSF = 190 mL) from USP-L for making hand sheets.

2.2. Production of (L)MFCs

(L)MFCs were produced by feeding pulp suspensions at 2 % solids into a SuperMassColloider (SMC, Model: MKZCA 6-2 J, Disk: MDGA 6-80#, Masuko Sangyo Co., Ltd., Japan) at 1500 rpm. The SuperMassColloider has two stone disks with the bottom disk rotating and the top disk stationary. The disk gap was initially set to zero without pulp (two disks just touch each other). The gap was then adjusted down to −100 μm after loading pulp. This disk gap was kept for all experiments. There was no direct contact between the two disks at this negative clearance due to the presence of pulp. These milling conditions were based on our earlier optimization study using the same BEP fibers (Hu et al., 2015). Disk grinding energies with and without pulp load were recorded by an energy meter. Approximately 100–200 g in oven dry weight pulp fibers were used in each fibrillation run. Each fiber suspension went through the SMC 1–4 passes in fibrillation. 800 mL of the fibrillated MFC suspension were taken out before each additional pass. The suspensions were stored in a refrigerator for further characterization. Energy consumptions for fibrillation at different passes were recorded. Total of 16 MFCs from 1 to 4 passes were produced from the 4 types of pulps. An extensively refined USP-L pulp with CSF of 190 mL was also produced using a Valley beater for comparison purpose.

2.3. Chemical composition analyses

The original pulps were ground to 30 mesh by a Wiley mill (Arthur H. Thomas Company, Model: 5XBG00B D, HP 1/4) for chemical composition determination by the conventional two-step concentrated sulfuric

acid hydrolysis with the hydrolysates analyzed by ion chromatography as described previously (Luo et al., 2010).

2.4. Optical microscopy and scanning electronic microscopy

Fibril samples from SMC were first characterized by OM imaging to provide the overall feature of the fibrillated cellulosic samples (Pöhler et al., 2010) and SEM imaging was performed to obtain details of the fibril dimensions. For OM, (L)MFC samples in water suspension were mounted without staining on microscope slides. Bright-field images were obtained with a Nikon Eclipse Ci microscope (Model number: 707484, Nikon Corp., Tokyo, Japan) equipped with an FLIR Grasshopper 3 camera.

For conventional SEM, a drop of MFC in water suspension was mounted on carbon tape over an aluminum stub and frozen in a freezer at −20 °C for 1 h. The samples were additionally frozen in liquid N_2, then transferred to a precooled freeze-drier at −60 °C and 200 mbar. The lyophilized samples were sputter-coated with gold, and secondary electron images were obtained at 10 kV accelerating voltage with a Zeiss Leo Evo 40 SEM system. To observe MFC in hydrated state by environmental SEM (ESEM), we used an FEI Quanta 200 SEM. Drops of MFC in water suspensions were mounted on carbon tape over specimen stubs. The observations were performed at 20 kV, and at relatively low vacuum of 3 Torr and 5 °C temperature.

2.5. Fiber quality and fine content analyses

The fiber quality and fine content are analyzed by a Fiber Quality Analyzer (FQA, LDA02, OpTest Equipment Inc., Canada). The FQA uses a circular polarized light to image cellulosic materials. Cellulosic fibers in aqueous suspension were fed into a flow cell that is imaged by circular polarized light with one polarizer and light source on one side of the flow cell and the second polarizer and camera on the opposite side, which enables a two-dimensional image of a cellulosic fibers displayed on a dark background because cellulose has birefringence. Thresholding the image using a gray level (GL) to result in a binary image that clearly shows the boundaries of the fibers or fibrils. The detection threshold is typically set between 9 and 11 GL while the GLs of the background image of the flow cell with one and both polarizers in place are approximately 1 and 140, respectively, which ensures images have a high contrast for accurate size determination.

The FQA tracker length software algorithm measures the length of fibers as they travel up the flow cell past the field of view. With pixel resolution of the camera at 7 μm × 14 μm, the minimal measurable length and width of fibers are at 70 μm and 7 μm, respectively. Fibers shorter than a preset limit can be defined as fines. For characterizing MFCs, measurements of fines (or short fibers) are most relevant and interesting. The fine contents are reported as the arithmetic mean count percentage of the total fibers tracked.

For the present study, the pulp solids concentrations in the suspensions were approximately 2 mg/L for softwood pulps USP-L and USP-H and 0.75 mg/L for hardwood pulps BEP and UHP, Concentration may vary slightly, but the fiber frequency is between at 20–90/eps in test process to ensure precision in results. For the four original pulps, disintegrator was used to disperse the fibers for FQA test because long fibers tend to get entangled. In each run, a total 5000 fibers and fines were counted to obtain statistical significance.

2.6. Water retention value (WRV) determination

WRVs of (L)MFCs and original pulp fibers were measured according to the Scandinavian test method SCAN-C 62:00 described in previous studies (Gu et al., 2018; Luo & Zhu, 2011). Each water saturated cellulosic fibril sol and fiber suspension of approximately 14 g at 2 % (the solids consistency after SMC fibrillation) were wrapped using a filtration membrane of pore size 0.1 μm (JVWP14225, Millipore Corporation, USA) and then put into a centrifuge tube supported by a stainless steel screen (Fig. S1) to leave space in the bottom of the tube for water accumulation during centrifugation (International Centrifuge EXD 4871, International Equipment Co., Chattanooga, TN, USA). The relative centrifuge force (RCF) is set as 3000*g* for 15 min.

The centrifuged cellulosic samples are weighed before and after oven drying at 105 °C to determine WRV as follows:

$$WRV(\%) = \frac{m_{wet} - m_{od}}{m_{od}} \times 100 \quad (1)$$

where "m_{wet}" in the equations is the mass of the wet cellulosic sample after centrifugation, and "m_{od}" is the mass of the wet cellulosic sample after oven drying.

To account for the effects of the physical and chemical structures of feedstock fibers on WRV, the normalized WRV (nWRV) of an MFC is defined as the measured MFC WRV divided by the WRV of the feedstock fibers used to produce the MFC. It is expected that nWRV can better represent the effect of fibrillation alone on MFC water retention.

$$nWRV = \frac{WRV_{MFC}}{WRV_{Feed\ Fibers}} \quad (2)$$

2.7. Suspension stability evaluation

(L)MFC suspension stability was evaluated by diluting all fibril suspensions to 0.25 wt% using DI water (Guimaraes, Botaro, et al., 2015). Uniform dispersion of a suspension was obtained by shaking and sonication. Fibril sedimentation of the dispersions in test tubes were observed by visual examination over time. Images of the dispersions were taken at 0, 1, 2, 3, 4, 5, 6, 7, 8 and 72 h. Suspension stability was calculated according to below equation (Silva et al., 2021a).

$$\text{Stability} = \left(\text{Dispersion height} / \text{Initial height} \right) \times 100 \quad (3)$$

where "Dispersion height" is the height of the dispersion at a given sedimentation time, and "Initial height" is the dispersion height before sedimentation occurring.

2.8. Cellulose crystallinity determination

Crystallinity was estimated by 380-Raman method (Agarwal et al., 2010; Agarwal et al., 2018), the LMFCs from 4 passes through SMC and their corresponding original pulps (3 kinds) except BEP, as well as the USP-L (190 mL CSF) were bleached with the chlorite treatment. The initial chemical charge was 300 mg sodium chlorite and 0.1 mL glacial acetic acid per g of dry wood pulp. The liquor to wood ratio was 15:l and the temperature of the water bath was 70 °C. The additional charge was added after 2, 4, and 6 h with 1 h of reaction after the last charge without withdrawal of any liquor (Ahlgren & Goring, 1971). The residual acid was washed with deionized water until the filtrate was neutral. The samples were dried in the hood-vent overnight for making pellets for Raman analysis. Samples were analyzed, in replicate using a Bruker MultiRam spectrometer (Bruker Instruments Inc. Billerica, MA). The Raman system is equipped with a 1064-nm 1000 mW continuous wave (CW) diode pumped Nd:YAG laser. Approximately 100 mg dry fibrillated-sample was pressed into a pellet (using ~276×10^6 dyn/cm^2 of compressive pressure from a hydraulic press) and Raman spectra were recorded from different pellet locations using 600 mW laser power. To obtain good signal-to-noise ratio, 2048 scans were averaged. For 380-Raman crystallinity estimation, the spectra were processed according to the previously reported method (Agarwal et al., 2010; Agarwal et al., 2018) The crystallinity standard deviation values are based on 2 spectral measurements, each consisting of 2048 averaged scans.

The bleached MFC pellets were also analyzed by wide-angle X-ray diffraction using a Bruker D8 Discover system with Cu–Ka radiation (Bruker Corp., Billerica, MA) at the Material Science Center, University

of Wisconsin, Madison, WI. The 2D detector of the system has a 14 cm diameter active area with a resolution of 2048 × 2048 pixels. A spot size of 0.5 mm was used. Scattering spectrum were collected in a 2 min period. XRD CrI were also calculated using the Seagal method (Segal et al., 1959) based on the scattering signals at 2θ = 18° and 22.7°:

$$CrI = 100 \times (I_{2\theta=22.7} - I_{2\theta=18})/I_{2\theta=22.7} \quad (4)$$

2.9. Papermaking and mechanical testing

The high kappa softwood pulp (USP-H) was refined to 600 mL CSF as the base fibers for making handsheets. 15 % of the base fibers were substituted with the LMFCs from the low kappa softwood pulp (USP-L) from each fibrillation passes 1–4 or a highly refined same USP-L at 190 mL CSF. Handsheets were made using well dispersed and diluted fibers and LMFC mixture suspension on a Manual Sheet Formers (The Hermann Manufacturing Co.). Total of 6 sets of handsheets with basis weight of 60 g/m^2 were made. Because no retention aid and white-water circulation were applied in sheet making, there were LMFC losses. Additional mixture of fiber and LMFC suspension was added to maintain the same sheet basis weight. As a result, the actual LMFC contents in sheets were estimated to be 13.6 %, 11.0 %, 9.4 %, 8.4 % with LMFCs of 1, 2, 3, 4 passes, respectively. The sheets were dried and conditioned at 70 °F and 50 % RH before mechanical testing using a horizontal tensile tester (Lorentzen & Wettre, Stockholm, Sweden). 10 paper strips of 15 mm wide and 120 mm long were cut from each set of handsheets for testing.

3. Results and discussion

3.1. Morphologies of (L)MFCs characterized by imaging

Optical microscopy can reveal the overall morphologies of (L)MFCs. As shown in Fig. 1, hardwood pulps (Fig. 1A0 and B0) have shorter and narrow fibers than softwood tracheids (Fig. 1C0 and D0). The hardwoods also contain vessel elements. As discussed in an earlier study (Wang, Zhu, et al., 2012), mechanical fibrillation through disk milling resulted in fibers delamination to break crosslinks between fibrils caused by compression driven internal fibrillation as well as external fibrillation caused by abrasive shear and friction forces to result in fiber shortening and producing hairs and fibrils on external surface (Hartman, 1985). This is clearly seen from Fig. 1 for all pulp samples. Increasing fibrillation duration resulted in increased degree of fiber fibrillation. This variation is dependent on pulp fiber type and on the amount of energy consumed in fibrillation as will be discussed in the following subsection. Visual observation indicates that for the low lignin softwood pulp sample (USP-L), one pass through the SMC (Fig. 1C1) already reached the similar degrees of fibrillation from 3 passes in the SMC for the other pulp samples (Fig. 1A3, B3, and D3).

Because of the limited spatial resolution in OM, SEM was also used with the focus on the fine details of the (L)MFC samples, especially the samples from the third and fourth passes. As shown in Fig. 2, Figs. S2 and S3A, after two passes through SMC, large fiber fragments remain in all samples (Fig. 2A2–D2). Fine fibrils on the order 100 nm appeared especially in the two hardwood samples (Fig. 2A2 and B2). An apparent increase in fibrillation was evident in the electron microscopy images after the second SMC pass of the hardwood samples (S3A). Increasing

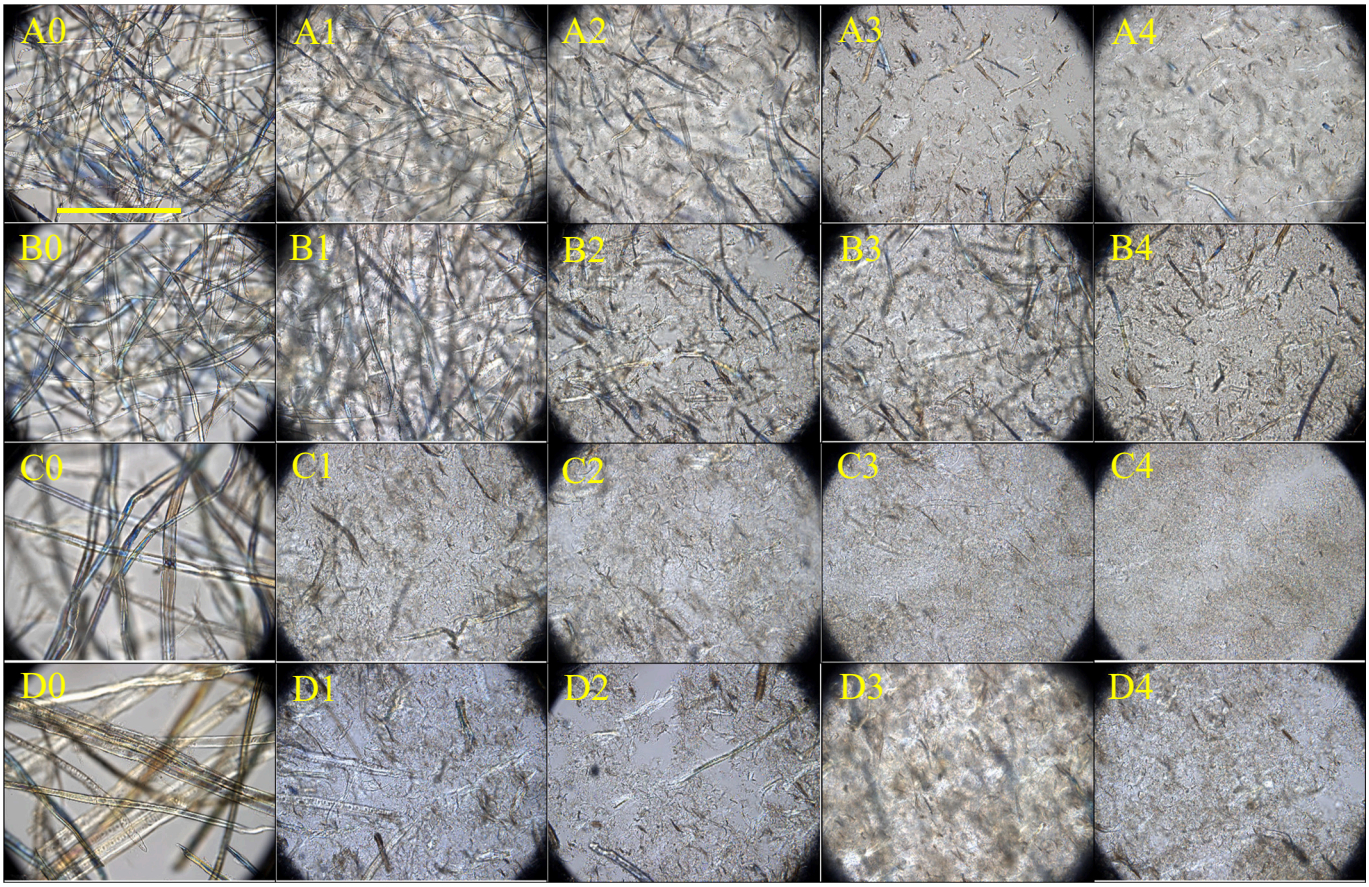

Fig. 1. Optical microscopic images of fiber/fibril samples. (A0–A4): Bleached eucalyptus kraft pulp (BEP); (B0–B4): Unbleached mixed hardwood kraft pulp (UHP); (C0–C4): Unbleached softwood kraft pulp-low lignin (USP-L); (D0–D4): Unbleached softwood kraft pulp-high lignin (USP-H). Scale = 500 μm for all images. Columns from left to right are original fibers, (L)MFCs with 1–4 passes through the SMC.

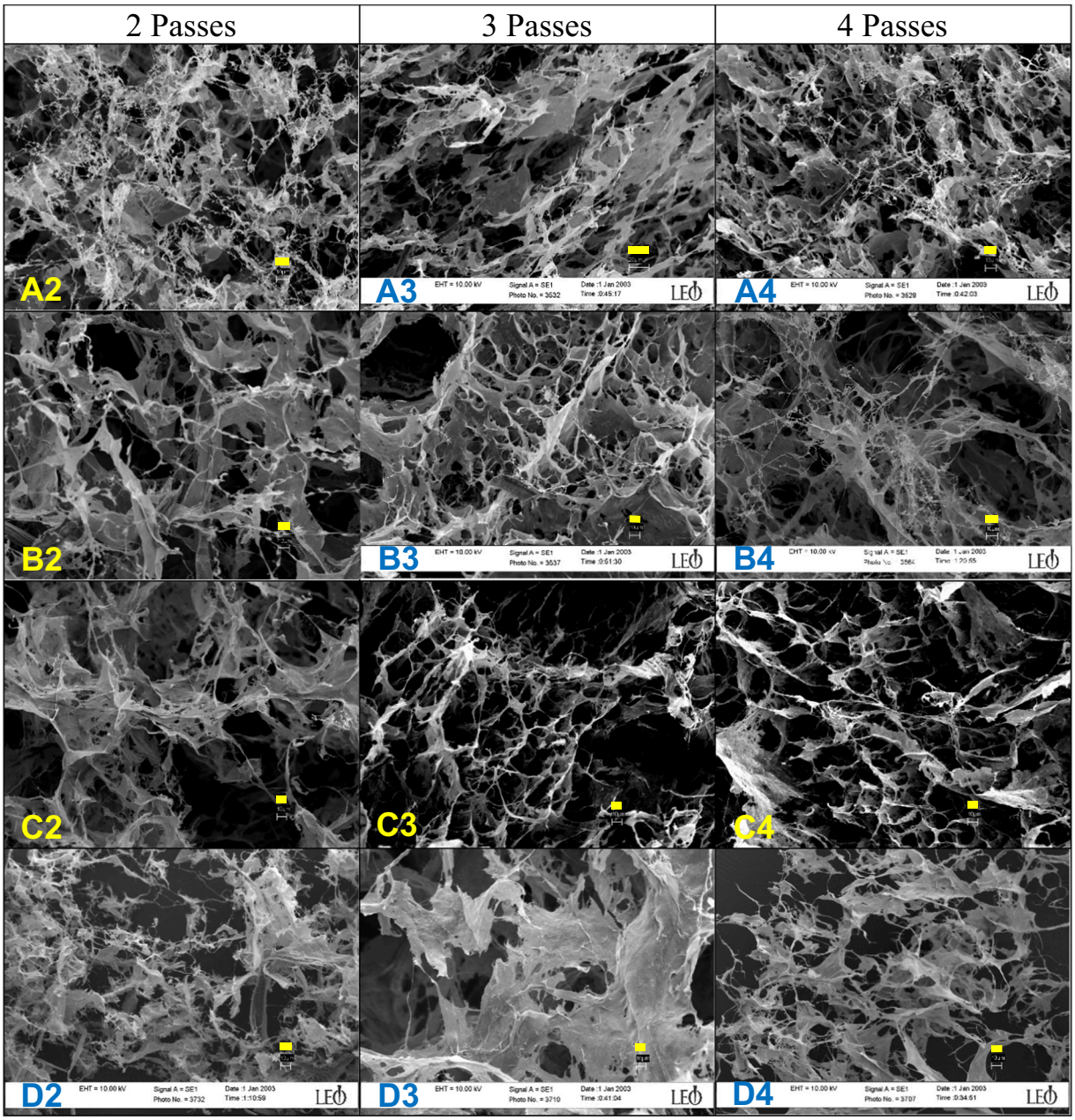

Fig. 2. Scanning electron microscopic images of LMFC samples. (A2–A4): Bleached eucalyptus kraft pulp (BEP); (B2–B4): Unbleached mixed hardwood kraft pulp (UHP); (C2–C4): Unbleached softwood kraft pulp-low lignin content (USP-L); (D2–D4): Unbleached softwood kraft pulp-high lignin content (USP-H). All scales = 10 μm except for A3 = 20 μm.

fibrillation by passing through SMC 3 passes, increased the delamination of the fiber fragments to became thin sheets. This is clearly seen from the BEP and USP-H pulp fibers (Fig. 2A3 and D3). After 4 passes through the SMC, these sheets were broken down and became smaller. The images showed that the two hardwood LMFCs (Fig. 2A4 and B4) had more nanoscale fibrils than the two softwood LMFCs (Fig. 2C4, D4, and Fig. S3B). Furthermore, it appears the USP-H sample with high lignin content is the most difficult to fibrillate with more large sheet fragments. The images also show that SMC is more effective in producing micro-scale fibrils or fragments than producing nanoscale fibrils. Applying 4 SMC passes on USP-L though significantly increased the energy as shown in Fig. 3, did not significantly improve its degree of fibrillation (comparing Fig. 2C3 and C4; and Fig. S2C3 with C4). Again, our observations suggest SMC has limited ability to generate significant nanofibrillation.

3.2. Fibrillation energy

It is well known that energy consumption for mechanical fibrillation of lignocellulosic fibers can be intensive and increases with increasing fibrillation time. Because fiber/fibril pulp suspensions were fed by gravity in the SMC, the amount of time for completing each pass varied with the friction force on the pulp suspension which depends on pulp samples and the stage (extent) of fibrillation, using the number of passes through the SMC is not a good measure to compare energy consumption for fibrillating different pulp samples. Here, we used the time required to fibrillate one kg fibers (min/kg) to examine fibrillation energy consumption. As shown in Fig. 3, fibrillation energy increased exponentially with fibrillation time. This suggests that (L)MFC surface area was increased exponentially because the energy was primarily spent on increasing (L)MFC surface area. It is noticed that energy consumption up

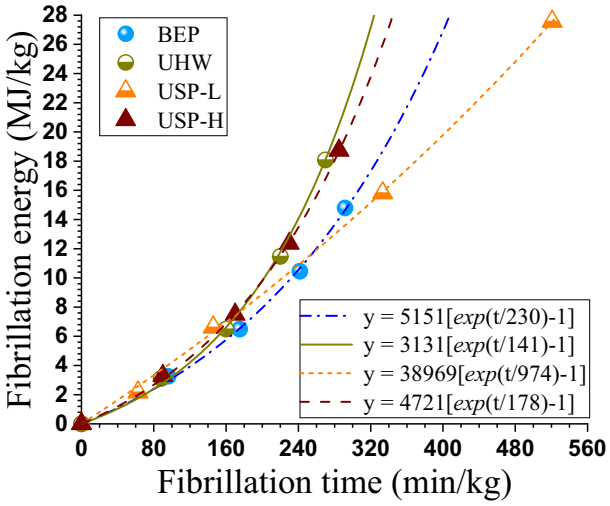

Fig. 3. Comparisons of fibrillation energy consumption among different pulp fibers.

to the second passes (microfibrillation based on the discussion from OM and SEM images), or fibrillation time of approximately 160 min/kg through the SMC was relatively lower of approximately 6.5 MJ/kg and falls to a single curve for all the 4 pulp fiber samples. However, the energy consumption data diverges for fibrillation beyond second passes. As discussed above in SEM image analysis, SMC is not effective in nanofibrillation which resulted in significant increase in energy consumption beyond second pass through SMC or entering the stage of nanofibrillation. Under the same fibrillation time, fibrillation energy was higher for UHP and USP-H than BEP and USP-L, as reflected from the slopes of the curves (Fig. 3). This suggests that the difference in cell wall chemical and physical structures mainly affect nanofibrillation. Earlie studies (Bian et al., 2017; Rojo et al., 2015) suggested that lignin can have a lubrication effect to facilitate cellulose fibrillation. The two softwood-pulp USP-L and USP-H were both from loblolly pine and were produced by the same mill with minor mixture of other species. However, the comparison of energy consumption between these two-pulp-derived LMFC samples suggests that high lignin content negatively affected nanofibrillation. This is likely due to the strong lignin glue effect at high lignin content, and the benefits of lubrication and radical scavenging ability of lignin may be limited to pulp fibers with low lignin content. Furthermore, SEM images show the LMFCs from USP-L is significantly finer than the corresponding LMFCs from USP-H (comparing Fig. 2C3 with D3, C4 with D4, and Fig. S2C3 with D3, C4 with D4).

3.3. Comparisons of (L)MFCs from different pulp samples

To provide an objective comparison among different pulp samples in terms of their relative resistance to fibrillation, one cannot simply compare the energy consumption alone, rather need to examine the extent of fibrillation as well, i.e., the efficiency of utilizing energy for creating surface. Visual observation of the OM images (comparing Fig. 1C2 with A2, B2, and D2, D3) indicates that much more surface area were created for USP-L than for the other three pulp samples through microfibrillation (two passes through SMC) at approximately the same fibrillation time of 160 min/kg or at approximately the same fibrillation energy of 6.5 MJ/ton (Fig. 3). These observations suggest that the unbleached softwood kraft pulp (low lignin content, bleaching grade), USP-L, is the least resistant to fibrillation. Comparison at extended fibrillation times (3 and 4 passes through the SMC, or nanofibrillation) is difficult due to the differences in fibrillation time and energy (Fig. 3). It should be pointed out that the SEM images were mainly focused on detecting the fine fibrils/structures and therefore not suitable for comparison of total surface area created, though coarse microfibers were also detected by SEM even after 4 passes through the SMC (Fig. S3B).

Quantitative comparison needs to be based on the total specific surface area created per unit of fibrillation energy input. This requires the ability to quantify the total specific surface area of the (L)MFCs – a very difficult task. Here we are trying to evaluate the ability of WRV measurements to characterize the degree of fibrillation of (L)MFCs and to compare (L)MFCs from different fiber sources. WRV is significantly affected by the chemical and physical structures of the fibers and varied significantly among different pulp samples. The measured WRVs were therefore normalized by the WRV of the corresponding unfibrillated pulp fibers (Eq. (2)). As shown in Fig. 4, nWRV of different MFCs increased with increasing fibrillation energy, suggesting comparisons of (L)MFCs with varied extent of fibrillation from the same pulp fibers can be made using nWRV. Despite the greater nWRV of a MFC from BEP than the corresponding value of the LMFC from UHP at the similar energy input, comparative conclusions on the degree of fibrillation among (L)MFCs from these fiber sources cannot be made because of the significant chemical and physical variations in the fiber sources (bleached eucalyptus vs mixed birch and maple). However, it appears that nWRV can be used to compare the extent of fibrillation of (L)MFCs from the two softwood pulp fibers despite the differences in their chemical structure due to varied extent of chemical pulping (delignification). These two softwood pulp samples were from the same wood species loblolly pine with slight variation in minor mixture, suggesting wood species is the dominant factor in affecting using nWRV for characterizing the extent of fibrillation of (L)MFCs. It appears that the nWRV values of the LMFCs from the USP-L pulp fibers plateaued after the second pass through the SMC. This could be attributed primary to the inefficient nanofibrillation by SMC which resulted in minor changes in the LMFCs nanostructure as can be seen from the SEM images (Fig. 2C2–C4). It may also suggest that nWRV is more sensitive to microfibrillated samples than to nanofibrillated samples.

The content of fine, a term used in the pulp paper industry to refer to the content of fibrils or short fibers, can be easily obtained by commercial fiber analyzers. Fiber Quality Analyzer (FQA) (Optest, ON, Canada) was used to determine the fine content of the (L)MFCs. To discern the fines in the original pulp samples (Fig. S4A–D), the increase in fine number content was used to qualitatively represent the amount of surface created through fibrillation. Because not all fines are the same in terms of length and width, data from two different fine length ranges

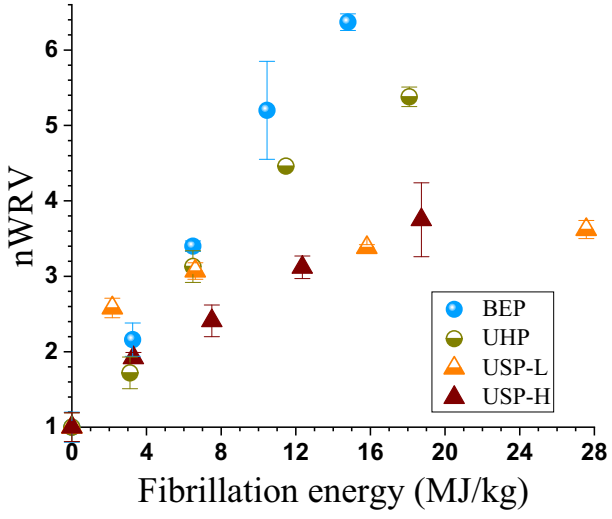

Fig. 4. Comparisons of normalized water retention value (nWRV) of various (L)MFCs produced from different fiber sources with different amount of fibrillation energy.

available on the instrument, 0.03–0.07 mm and 0.07–0.2 mm, were used. As shown in Fig. S5, fines content increased with fibrillation energy for MFCs from all pulp fibers. USP-L had the most increase in fine content of 0.03–0.07 mm size (Fig. S5A), while BEP has the most increase in the fine content of 0.07–0.2 mm size (Fig. S5B). This may suggest that USP-L is easier to fibrillate than BEP and the other pulp samples, a conclusion in agreement with the discussion presented earlier using the imaging analyses. It appears that fines number content can be a measure of the extent of fibrillation for (L)MFCs, but in general, it is difficult if used to compare (L)MFCs from different fiber sources. It is also noted that the fines 0.03–0.07 mm number content for USP-L plateaued after 3rd passes, perhaps due to the insensitivity of FQA in detecting the nanoscale fibrils, or alternatively, SMC is not effective in producing nanoscale fibrils as discussed earlier. The increase in fines content is also reflected from the reduction of fiber length (>0.07 mm) as shown in Fig. S5C. Again comparisons cannot be made between samples from different fiber sources. The two softwood pulps with much longer initial fiber length had much greater decreases in the length weighted fiber length (Lw) than the two hardwood pulp samples.

It is well known that nanofibrillation of cellulosic fibers can result in a colloidally stable suspension, or gelation. Therefore, the stability of MFC suspensions can be a measure of the extent of fibrillation as illustrated in earlier studies for MFCs from the same bleached fibers (Guimaraes, Botara, et al., 2015; Silva et al., 2021b). Whether or not suspension stability can be used to compare (L)MFCs from different (bleached and unbleached) fibers was evaluated here. Fig. 5 shows the

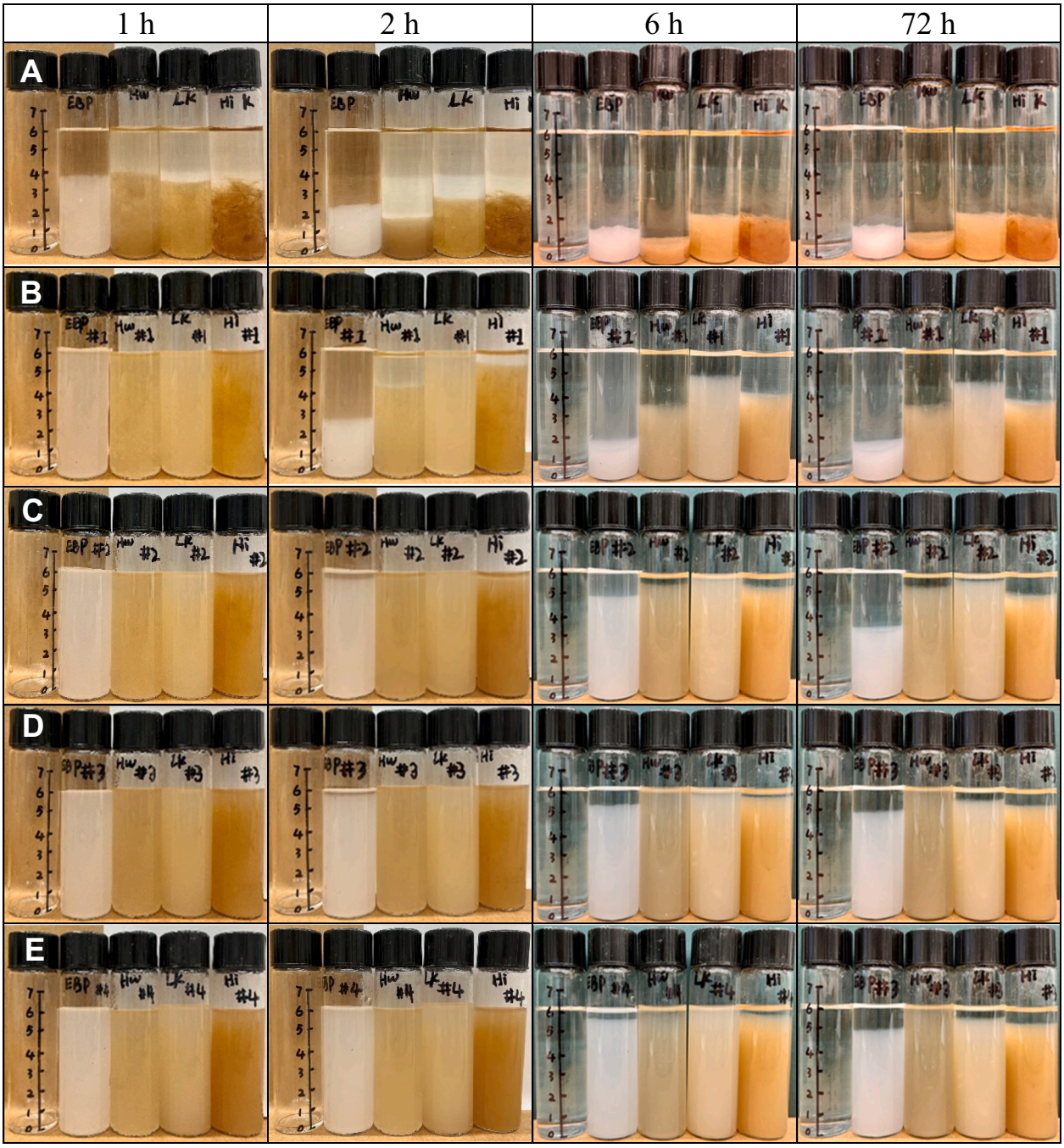

Fig. 5. Images of suspensions of various fibers (A) and their (L)MFCs from different passes: (B) 1 pass, (C) 2 passes, (D) 3 passes, (E) 4 passes, through the SMC taken from different standing times.

suspension images of different types of fibers and their (L)MFCs taken from various standing times upto 72 h. The images show that the unfibrillated fibers (Fig. 5A, row A) settled very quickly, while the nanofibrillated samples (3 and 4 passes through the SMC) shown in Fig. 5D and E appeared very stable with minimal sedimentation even after standing for 72 h, suggesting sufficient fibrillation resulted in stable sols. This also suggests that the strong interaction with water due to the substantially increased fibril surface area with extended- or nanofibrillation, made suspension stability not a sensitive (good) measurer to characterize the degree of fibrillation. Fortunately, suspension stability can be a good measurer of the degree of fibrillation for MFCs with low to medium level of microfibrillation (1 and 2 passes through the SMC) as shown in Fig. 5B and C.

The stabilities of the MFC suspensions were calculated according to Eq. (3) based on the sedimentation height on the captured images as shown in Fig. 5. Again, the MFCs from 3 and 4 passes through the SMC showed very high stability and the data were not sensitive to variation among samples. However, the stability of the MFCs from 1 and 2 passes through SMC varied from 0.3 to 0.9 (Fig. 6). We ranked these (L)MFCs from different pulp samples using the suspension stability. We choose standing time 2 and 6 h as listed in Table 1. We compared with the fineness rank using visual observation based on OM imaging (Fig. 1). As listed in Table 1, in general, the stability ranking is in agreement with the ranking based on visual observations, except for samples UHP-P2 and USP-H-P1. It appears wood physical structure and chemical composition can affect (L)MFC suspension stability to cause suspension stability rankings deviation from the rankings based on OM visual observations.

3.4. Crystallinity measurements

The Raman crystallinity data for the (L)MFCs along with their respective controls are reported in Table 2. For BEP derived MFCs, the crystallinity of the fibers declined significantly (30 %), from 53.7 to 37.6 %, although CrI of BEP-P3 was slightly higher compared to BEP-P2

Table 1
Ranking of (L)MFCs based on OM imaging, their suspension stability.

Sample[a]	S (t = 2 h)	S (t = 6 h)	Visual rank	S (t = 2 h) rank	S (t = 6 h) rank
BEP-P1	0.479	0.304	7	8	8
BEP-P2	0.938	0.786	5	4	4
UHP-P1	0.708	0.571	8	7	7
UHP-P2	0.958	0.929	6	2	2
USP-L-P1	0.917	0.821	2	5	5
USP-L-P2	0.992	0.964	1	1	1
USP-H-P1	0.875	0.679	4	6	6
USP-H-P2	0.958	0.929	3	2	2

[a] Pn stands for numbers of pass through the SMC.

(respectively, 41.8 and 37.9 %; Table 2). The reason for this not clear but overall, pulp fibrillation seems to be the reason why significant decrystallization occurred. Similarly, in the case of UHP pulp, due to the SMC treatment, the pulp CrI was reduced from 50.2 (control) to 46.9 % (UHP-P4), which is three times smaller decline (9.3 %) compared to the decline seen in BEP fibers (30 %). However, once again, an anomaly was observed in the data – compared to the CrI of UHP-P4, the CrI of UHP-P2 was lower (40.3 %) and the CrI of UHP-P3 was slightly higher (51.1 %) than UHP (50.2), which was the control pulp. However, based on decrystallization role of SMC, the expectation was that the cellulose in UHP-P4 and UHP (control) should have been, respectively, least and most crystalline. On the contrary, a more regular pattern of crystallinity change was observed for the USP-L pulp. In this case, after 4 passes in the SMC, the control pulp's CrI declined from 51 % to 42.1 % (Table 2), a decline of 17.5 %. The slightly lower value of the sample USP-L-P3 (40.4 %) compared to 42.1 % of USP-L-P4, is within the experimental error (SD 5.7 %, Table 2). When the Valley beater processed pulp (USP-L-VB) was compared to the control (USP-L) (Fig. S6), a significant reduction in the CrI was observed (decline of 15 %, Table 2) which was similar to the decline seen for USP-L-P4 (17.5 %). The last MFC set in Table 2, USP-H

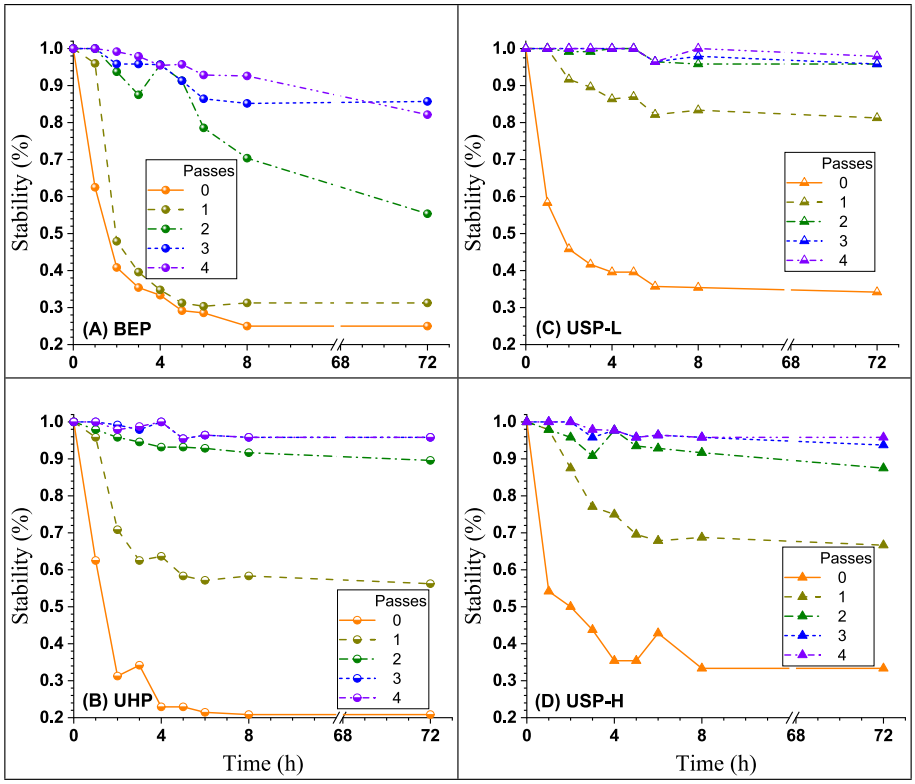

Fig. 6. Stability of suspensions of various fibers and their (L)MFCs.

Table 2
Crystallinity of the (L)MFCs.

Sample[a]	380-Raman CrI (%)	ΔCrI/CrI (%)	XRD CrI (%)	ΔCrI/CrI (%)
BEP	53.7		83.1	
BEP-P1	47.8	−11.0	80.4	−3.2
BEP-P2	37.9	−29.4	75.3	−9.4
BEP-P3	41.8	−22.2	81.5	−1.9
BEP-P4	37.6	−30.0	73.2	−11.9
UHP	50.2		83.5	
UHP-P1	46.7	−7.0	81.4	−2.5
UHP-P2	40.3	−19.7	84.5	1.2
UHP-P3	51.1	1.8	90.0	7.8
UHP-P4	46.9	−6.6	79.0	−5.4
USP-L	51		84.0	
USP-L-P1	50.3	−1.4	83.1	−1.1
USP-L-P2	47.3	−7.3	82.5	−1.8
USP-L-P3	40.4	−20.8	82.3	−2.0
USP-L-P4	42.1	−17.5	89.9	7.0
USP-L-VB[b]	43.4	−14.9	83.1	−1.1
USP-H	50.2		79.2	
USP-H-P1	49.5	−1.4	89.7	13.3
USP-H-P2	55.7	11.0	87.8	10.9
USP-H-P3	46.1	−8.2	84.3	6.4
USP-H-P4	52.9	5.4	90.5	14.3

[a] Pn stands for numbers of pass through the SMC.
[b] Valley beater treated pulp at 190 mL CSF.

to USP-H-P4, did not show a particular trend and the CrI data varied significantly (46.1 to 55.7 %). Although the Raman CrI data had some anomalies, considering that the samples were analyzed in dry state, the former may be a result of sample drying. Therefore, it would be of interest to investigate this aspect further by obtaining CrIs of MFCs in the never-dried state. The justification being that drying would cause the collapse of the SMC-generated fibrils which is likely to impact, in some way, the crystallinity measurement.

CrI data from XRD performed substantially poorer than Raman CrI as listed in Table 2 for ranking the extent of fibrillation of the (L)MFCs except for the BEP sample with similar trends as those observed in Raman CrI.

3.5. Paper mechanical testing analysis

Handsheets made of lightly under-refined (CSF = 600 mL) USP-H pulp fibers were substituted with 15 % different LMFCs from USP-L and a highly refiner (CSF = 190 mL) USP-L-VB. As stated in the experimental section, the actual LMFC contents were 13.6 %, 11.0 %, 9.4 %, 8.4 % in the sheets with LMFCs of 1, 2, 3, 4 passes, respectively. The results show that handsheets tensile strength was increased (Fig. S7), however tensile modulus and failure strain increases were minimal. Moreover, the finer LMFCs from more passes through SMC were as effective as the more course MFCs in enhancing sheet tensile strength but at a reduced MFC loadings. It appears that the highly refined USP-L pulp was also very effective in improving handsheets tensile strength than all LMFCs.

4. Conclusions

Several conclusions can be drawn from the present study: (1) Characterizing the morphology of (L)MFCs is extremely difficult. Comparisons of (L)MFCs derived from different wood pulps was not possible by several methods evaluated in this study, such as cellulose crystallinity, water retention value (WRV), and fines content. Techniques based on water interactions seemed can provide some degree of assessment of MFCs. Wood physical structure has a significant impact on WRV of (L)MFCs. However, WRV can be used to compare (L)MFCs from the same wood fibers. (2) For microfibrillation, such as 1 and 2 passes through the SuperMassColloider (SMC) in the present study, the energy consumption is low. Furthermore, energy consumption used for microfibrillation among different wood fibers was not much different over time. Nevertheless, it appears that (L)MFC suspension stability is a pretty good measure for comparing coarse (L)MFCs (with 1 or 2 passes from SMC) from different wood fibers, based on visual ranking using optical microscopy. (3) The SMC used in the present study is not efficient for nanofibrillation. (4) Based on the four wood pulp samples evaluated, the low lignin content softwood pulp is the easiest to fibrillate (microfibrillation or 1 and 2 passes through the SMC). However, further fibrillation beyond 2 passes, or nanofibrillation is not effective by the SMC.

CRediT authorship contribution statement

Zhang conducted LMFC production and characterization by optical microscopy imaging, WRV, fine content, and stability test, handsheet properties, and draft the manuscript. **Kitin** conducted SEM imaging. **Gleisner** helped LMFC production. **Agarwal** conducted Raman CrI measurements. **Zhu** secured pulp fibers, designed experiments, directed the study, data analysis, and significantly contributed to the writing and edited the manuscript.

Declaration of competing interest

The authors declare that they do not have competing interests for the work reported here.

Data availability

Data will be made available on request.

Appendix A. Supplementary data

Supplementary data to this article can be found online at https://doi.org/10.1016/j.carbpol.2023.120996.

References

Agarwal, U. P. (2022). Beyond crystallinity: Using Raman spectroscopic methods to further define aggregated/supramolecular structure of cellulose. *Frontiers in Energy Research, 10*.

Agarwal, U. P., Ralph, S. A., Reiner, R. S., & Baez, C. (2018). New cellulose crystallinity estimation method that differentiates between organized and crystalline phases. *Carbohydrate Polymers, 190*, 262–270.

Agarwal, U. P., Reiner, R. R., & Ralph, S. A. (2013). Estimation of cellulose crystallinity of lignocelluloses using near-IR FT-raman spectroscopy and comparison of the Raman and Segal-WAXS methods. *Journal of Agricultural and Food Chemistry, 61*(1), 103–113.

Agarwal, U. P., Reiner, R. S., & Ralph, S. A. (2010). Celulose I crystallinity determination using FT-raman spectroscopy: Univariate and multivariate methods. *Cellulose, 17*(4), 721–733.

Ahlgren, P. A., & Goring, D. A. I. (1971). Removal of wood components during chlorite delignification of black spruce. *Canadian Journal of Chemistry, 49*(8), 1272–1275.

Bian, H., Chen, L., Dai, H., & Zhu, J. Y. (2017). Integrated production of lignin containing cellulose nanocrystals (LCNC) and nanofibrils (LCNF) using an easily recyclable dicarboxylic acid. *Carbohydrate Polymers, 167*, 167–176.

Butchosa, N., & Zhou, Q. (2014). Water redispersible cellulose nanofibrils adsorbed with carboxymethyl cellulose. *Cellulose, 21*(6), 4349–4358.

Gu, F., Wang, W., Cai, Z., Xue, F., Jin, Y., & Zhu, J. Y. (2018). Water retention value for characterizing fibrillation degree of cellulosic fibers at micro and nanometer scales. *Cellulose, 25*(5), 2861–2871.

Guimaraes, M., Jr., Botara, V. R., Novack, K. M., Neto, W. P. F., Mendes, L. M., & Tonoli, G. H. D. (2015a). Preparation of cellulose nanofibrils from bamboo pulp by mechanical defibrillation for their applications in biodegradable composites. *Journal of Nanoscience and Nanotechnology, 15*(9), 6751–6768.

Guimaraes, M., Jr., Botaro, V. R., Novack, K. M., Neto, W. P., Mendes, L. M., & Tonoli, G. H. (2015b). Preparation of cellulose nanofibrils from bamboo pulp by mechanical defibrillation for their applications in biodegradable composites. *Journal of Nanoscience and Nanotechnology, 15*(9), 6751–6768.

Hartman, R. R. (1985). Mechanical treatment of pulp fibers for paper property development. In *The 8th fundamental research symposium: papermaking raw materials Oxford* (pp. 413–442). England Mechanical Engineering Publications Limited.

Hu, C., Zhao, Y., Li, K., Zhu, J. Y., & Gleisner, R. (2015). Optimizing cellulose fibrillation for the production of cellulose nanofibrils by a disk grinder. *Holzforchung, 69*(8), 993–1000.

Kaeb, H., & General, S. (2009). Bioplastics bioplastics: Technology, markets, policies. In *4th European bioplastics conference, Berlin* (pp. 10–11).

Kangas, H., Lahtinen, P., Sneck, A., Saariaho, A.-M., Laitinen, O., & Hellén, E. (2014). Characterization of fibrillated celluloses. A short review and evaluation of characteristics with a combination of methods. *Nordic Pulp Paper Res. J., 29*(1), 129–143.

Klemm, D., Kramer, F., Moritz, S., Lindstrom, T., Ankerfors, M., Gray, D., & Dorris, A. (2011). Nanocelluloses: A new family of nature-based materials. *Angewandte Chemie (International Ed. in English), 50*(24), 5438–5466.

Laitinen, O., Kemppainen, K., Stoor, T., & Niinimäki, J. (2011). Fractionation of pulp and paper particles selectively by size. *BioResources, 6*(1), 672–685.

Laitinen, O., & Niinimaki, J. (2014). Fractional study of the microfibrillated cellulose. *Tappi Journal, 13*(7), 49–55.

Lavoine, N., Desloges, I., Dufresne, A., & Bras, J. (2012). Microfibrillated cellulose - Its barrier properties and applications in cellulosic materials: A review. *Carbohydrate Polymers, 90*(2), 735–764.

Li, T., Chen, C., Brozena, A. H., Zhu, J. Y., Xu, L., Driemeier, C., Dai, J., Rojas, O. J., Isogai, A., Wågberg, L., & Hu, L. (2021). Developing fibrillated cellulose as a sustainable technological material. *Nature, 590*(7844), 47–56.

Luo, X., Gleisner, R., Tian, S., Negron, J., Horn, E., Pan, X. J., & Zhu, J. Y. (2010). Evaluation of mountain beetle infested lodgepole pine for cellulosic ethanol production by SPORL pretreatment. *Industrial and Engineering Chemistry Research, 49*(17), 8258–8266. https://doi.org/10.1021/ie1003202

Luo, X., & Zhu, J. Y. (2011). Effects of drying-induced fiber hornification on enzymatic saccharification of lignocelluloses. *Enzyme and Microbial Technology, 48*(1), 92–99.

Moon, R. J., Hensdal, C. L., Beck, S., Fall, A., Costa, J., Kojima, E., Abitbol, T., Raghuwanshi, V., Walker, C., & Batchelor, W. (2023). Setting priorities in CNF particle size measurement: What is needed vs. what is feasible. *TAPPI J., 22*(2), 116–137.

Nassiri, S., Chen, Z., Jian, G., Zhong, T., Haider, M. M., Li, H., Fernandez, C., Sinclair, M., Varga, T., Fifield, L. S., & Wolcott, M. (2021). Comparison of unique effects of two contrasting types of cellulose nanomaterials on setting time, rheology, and compressive strength of cement paste. *Cement and Concrete Composites, 123*.

Perkins, E. L., & Batchelor, W. J. (2012). Water interaction in paper cellulose fibres as investigated by NMR pulsed field gradient. *Carbohydrate Polymers, 87*(1), 361–367.

Pöhler, T., Lappalainen, T., Tammelin, T., Eronen, P., Hiekkataipale, P., Vehnisinen, A., & Koskinen, T. M. (2010). Influence of fibrillation method on the character of nanofibrillated cellulose (NFC). In *, 22. TAPPI 2010 international conference on nanotechnology for the forest products industry 1 Dec 2010*.

Raj, T., Kapoor, M., Semwal, S., Sadula, S., Pandey, V., Gupta, R. P., Kumar, R., Tuli, D. K., & Das, B. P. (2016). The cellulose structural transformation for higher enzymatic hydrolysis by ionic liquids and predicting their solvating capabilities. *Journal of Cleaner Production, 113*, 1005–1014.

Rojo, E., Peresin, M. S., Sampson, W. W., Hoeger, I. C., Vartiainen, J., Laine, J., & Rojas, O. J. (2015). Comprehensive elucidation of the effect of residual lignin on the physical, barrier, mechanical, and surface properties of nanocellulose films. *Green Chemistry, 17*, 1853–1866.

Saito, T., Nishiyama, Y., Putaux, J. L., Vignon, M., & Isogai, A. (2006). Homogeneous suspensions of individualized microfibrils from TEMPO-catalyzed oxidation of native cellulose. *Biomacromolecules, 7*(6), 1687–1691.

Segal, L., Creely, J. J., Martin, A. E., & Conrad, C. M. (1959). An empirical method for estimating the degree of crystallinity of native cellulose using the X-ray diffractometer. *Textile Research Journal, 29*, 786–794.

Silva, L. E., Dos Santos, A. A., Torres, L., McCaffrey, Z., Klamczynski, A., Glenn, G., Sena Neto, A. R., Wood, D., Williams, T., Orts, W., Damasio, R. A. P., & Tonoli, G. H. D. (2021a). Redispersion and structural change evaluation of dried microfibrillated cellulose. *Carbohydrate Polymers, 252*, Article 117165.

Silva, L. E., dos Santos, A. D. A., Torres, L., McCaffrey, Z., Klamczynski, A., Glenn, G., Sena Neto, A. R. D., Wood, D., Williams, T., Orts, W., Damásio, R. A. P., & Tonoli, G. H. D. (2021b). Redispersion and structural change evaluation of dried microfibrillated cellulose. *Carbohydrate Polymers, 252*.

Singh, M., Pahal, V., & Ahuja, D. (2020). Isolation and characterization of microfibrillated cellulose and nanofibrillated cellulose with "biomechanical hotspots". *Carbohydrate Polymers, 234*, Article 115827.

Siró, I., & Plackett, D. (2010). Microfibrillated cellulose and new nanocomposite materials: A review. *Cellulose, 17*, 459–494.

Turbak, A. F., Snyder, F. W., & Sandberg, K. R. (1983). Microfibrillated cellulose, a new cellulose product: Properties, uses, and commercial potential. *Journal of Applied Polymer Science: Applied Polymer Symposium, 37*, 815–827.

Wang, Q. Q., He, Z., Zhu, Z., Zhang, Y.-H. P., Ni, Y., Luo, X. L., & Zhu, J. Y. (2012a). Evaluations of cellulose accessibilities of lignocelluloses by solute exclusion and protein adsorption techniques. *Biotechnology and Bioengineering, 109*(2), 381–389.

Wang, Q. Q., Zhu, J. Y., Gleisner, R., Kuster, T. A., Baxa, U., & McNeil, S. E. (2012b). Morphological development of cellulose fibrils of a bleached eucalyptus pulp by mechanical fibrillation. *Cellulose, 19*(5), 1631–1643.

Weiss, N. D., Felby, C., & Thygesen, L. G. (2018). Water retention value predicts biomass recalcitrance for pretreated lignocellulosic materials across feedstocks and pretreatment methods. *Cellulose, 25*(6), 3423–3434.